Climate Dynamics
https://doi.org/10.1007/s00382-024-07258-3

ORIGINAL ARTICLE

Incorporation of RCM-simulated spatial details into climate change projections derived from global climate models

Kimmo Ruosteenoja[1] · **Jouni Räisänen**[2]

Received: 28 November 2023 / Accepted: 26 April 2024

Abstract
Regional climate models (RCMs) exhibit greater potential than global models (GCMs) in capturing geographical details of climate change arising from orography and land–water distribution, but dynamical downscalings are only available for a limited number of GCMs. The full GCM ensembles are much more representative. Furthermore, the current EURO-CORDEX RCM runs most likely underestimate future warming. Thus, neither GCMs nor RCMs as such constitute an ideal tool for preparing reliable spatially detailed climate projections. This study introduces an easy-to-use GCM-RCM hybrid method that takes advantage of the best properties of both model categories. The large-scale response is adopted from GCM simulations, but the pattern is enriched with RCM-simulated details. For temperature projections, the procedure resembles the conventional pattern-scaling technique. However, the spatial averages of temperature change used for scaling are calculated over an area surrounding each grid point, either by giving an equal weight to the entire area or by taking into account the land–sea distribution. For precipitation, a linearised version of the method has been formulated. The method is demonstrated by integrating spatial details from 12 EURO-CORDEX RCM simulations with the CMIP6 multi-GCM mean projection. The resulting temperature responses include RCM-generated spatial details of up to ~ 1 °C while effectively correcting the general tendency of RCMs to underestimate warming in Europe. For precipitation, geographical details originating from the different CORDEX runs tend to diverge, resulting in a low signal-to-noise ratio. This probably reflects the substantial impact of internal variability on small-scale changes in precipitation.

Keywords Climate change · GCM-RCM hybrid method · CMIP6 · EURO-CORDEX · Temperature · Precipitation

1 Introduction

Projections of future climate change have been widely derived from both global and regional climate models (GCMs and RCMs) (IPCC 2021). Both model categories have their benefits and drawbacks.

GCMs offer a broad range of more or less independent simulations, but they are unable to resolve fine-scale regional details of change caused by, for example, orographic variations and the distribution of land, sea and inland water bodies (Jacob et al. 2014; Torma et al. 2015; Giorgi et al. 2016). For example, GCMs barely discern the impact of the Alps and the Baltic Sea on the future temperature response (Fig. 1a, c), whereas RCMs can simulate such small-scale features in much more detail (Fig. 1b, d). On the other hand, the currently used European Coordinated Regional Downscaling Experiment (EURO-CORDEX) RCM runs (Jacob et al. 2014, 2020) that have been used to downscale the Coupled Model Intercomparison Project Phase 5 (CMIP5) GCM simulations tend to simulate much weaker future warming than their driving GCMs, especially in summer; this is evidently due to deficiencies in the implementation of the RCM simulations (Boé et al. 2020a). According to Coppola et al. (2021, Fig. 1), CORDEX RCMs exhibit a weaker warming response for summer in comparison to the CMIP5 and, in particular, the CMIP6 ensemble. Figure 1 illustrates that, in two European example sub-regions, warming is likewise much weaker in the sub-ensemble of 12 CORDEX RCM runs considered here (defined in Sect. 2) than in the

✉ Kimmo Ruosteenoja
kimmo.ruosteenoja@fmi.fi

Jouni Räisänen
jouni.raisanen@helsinki.fi

[1] Finnish Meteorological Institute, P.O. Box 503, 00101 Helsinki, Finland

[2] Institute for Atmospheric and Earth System Research, University of Helsinki, P.O.Box 64, 00014 Helsinki, Finland

Published online: 20 June 2024

CMIP6 GCM runs. Furthermore, the representativeness of the RCM runs is typically low. Only a few driving GCMs have been used to provide boundary data, generally using a single realization for each GCM, and the simulations are not independent, because many of them share either the same RCM or the same driving GCM. Accordingly, neither set of models as such is an ideal basis for preparing future climate projections.

In this study, the solution to the aforementioned issues is sought by (1) extracting the general level and large-scale distribution of changes from GCM simulations but (2) incorporating regional details inherited from RCM runs in the response. The applicability of the developed GCM-RCM hybrid method in simulating changes in mean temperature and precipitation in Europe is investigated. The technique is straightforward and user-friendly; for example, no sophisticated statistical analyses are required, and simulation data are only needed at monthly time resolution.

Jacob et al. (2020) underlines that cooperation between the RCM and GCM communities should be strengthened by overcoming institutional, disciplinary and philosophical barriers that often exist between the clusters. The current study aims, from its specified perspective, to build a bridge between the two categories of models.

Taranu et al. (2023) suggest that the primary source of failure of the EURO-CORDEX RCMs in simulating sufficient degree of future warming is the misrepresentation of key physical processes affecting climate, in particular the lack of anticipated decrease in aerosol forcing, but also omission of the increasing stomatal resistance of plants due to higher CO_2 concentrations. Inconsistencies in the parameterization of sub-grid scale phenomena in the GCMs and RCMs constitute yet another potential factor that may degrade regional simulations. By the end of this century, EURO-CORDEX RCMs tend to simulate summer warming that is 1.5–2 °C weaker than in the driving GCMs (Boé et al. 2020a). Moreover, in Central Europe precipitation does not decrease as much as in the GCM runs, and incident solar radiation at the surface even decreases, in contrast to an increase in CMIP5 and CMIP6 GCM simulations (Coppola et al. 2021). Owing to these shortcomings, Boé et al. (2020a) recommend that EURO-CORDEX simulations should not be used as the single source for future climate projections. Such an approach would entail major risks of ignoring the worst-case hot-dry scenario, that is, the possibility that future warming in Europe would be strong and accompanied by a substantial reduction in precipitation.

In particular, it is the added value of RCM simulations in projecting large-scale long-term mean changes that is questionable (Taranu et al. 2023; Jacob et al. 2020, and references therein). Conversely, Lenderink et al. (2023) suggest that small-scale regional features in the mean temperature response simulated by RCMs may be plausible, even though the corresponding details in precipitation change are less robust when compared to natural variability.

In addition to standard RCMs, dynamical downscalings have been carried out using very high-resolution Convection Permitting Models (CPMs). In CPMs the grid spacing is typically <5 km, which makes the models computationally highly demanding (e.g. Erlandsen et al. 2020; Lind et al. 2023). As a result, CPMs can only be used to downscale a very limited number of GCM runs. Thus, for a long time to come, there will be a need to generalise those few fine-scale downscalings to represent wider GCM ensembles (Erlandsen et al. 2020).

We found a few previous studies utilising different techniques to combine the output of RCMs and GCMs for constructing spatially detailed climate change scenarios. Lenderink et al. (2007) prepared such scenarios for the Netherlands by decomposing the climate response into components driven by global warming and changes in the mean westerly flow in Europe. The local change was assessed by determining how selected climate indices responded to these changes in RCM experiments. Ruosteenoja et al. (2011) derived the temperature accumulation of future growing seasons in Finland from CMIP3 GCMs, but to conduct a sensitivity analysis, the GCM-based response was subsequently modified by regional details inferred from contemporary RCM data.

Li et al. (2012) utilised linear regression to establish links between the local temperature responses simulated by RCMs and the corresponding driving GCM, and these relations were applied to emulate downscaled responses for a large ensemble of GCM simulations. The resulting surrogate downscalings were used to determine probability distributions of mean temperature increase for North America at a high resolution. Olesen et al. (2018) employed a regression model to explain interannual variations in RCM-simulated climate indices (e.g., the length of the thermal growing season in Southern Greenland) by annual mean temperature in the driving GCM simulation. The regression equation was applied to convert the uncertainty range of warming projected by the CMIP5 GCMs into the uncertainty of the indices.

Erlandsen et al. (2020) devised a variant of statistical regional downscaling in which the geographical distributions of weather variables generated by a GCM, represented by empirical orthogonal function expansions, were used to predict the corresponding RCM-simulated distributions for Southern Norway. The resulting regression coefficients can then be used to establish fine-scale projections for those GCMs which have not been downscaled by that RCM. A similar idea was employed by Boé et al. (2023), who likewise applied statistical downscaling to GCM output data using RCM simulations rather than observations. Analogues for a meteorological field simulated by a GCM were first

sought on a coarse grid from the output of the corresponding RCM downscaling, and a linear combination of the analogues on a fine grid provided a spatially detailed estimate for the meteorological variable over Western Europe. For example, this technique involves the benefit that the ensuing fine-scale projections are unaffected by the underestimation of summer warming in the EURO-CORDEX RCM simulations.

The present study is structured as follows. The GCM and RCM data are described in Sect. 2. Section 3 introduces two variants of the GCM-RCM hybrid method that are used to produce spatially detailed climate projections by extracting the large-scale response from GCMs and fine-scale details from RCM simulations. In the results Sect. 4 we assess the applicability of the hybrid method for mean temperature and precipitation projections. The paper is finalised by the Discussion and Conclusions Sects. 5 and 6.

2 Model data

In this study, we analysed 12 EURO-CORDEX-11 RCM runs listed in Table 1. Considering all these runs, the total number of both different RCMs and driving CMIP5 GCMs providing boundary conditions is five. The number of runs ranges from 1 to 4 for a CORDEX model and from 1 to 3 for a driving GCM (Table 1). The grid spacing in the simulations is approximately 12 km (Jacob et al. 2014).

The GCM dataset consists of 28 CMIP6 models, each with 1–10 parallel runs (Supplement Table S1). The grid spacing in these GCMs is much coarser than in the CORDEX-11 RCMs, typically varying between 100 and 200 km depending on the model. For both the RCMs and GCMs, we analysed the time series of monthly mean near-surface air temperature and precipitation. The data were extracted from historical model runs up to 2014 for CMIP6 GCMs and 2005 for CORDEX RCMs. Thereafter, for the CMIP6 models, the mid-range Shared Socioeconomical Path SSP2-4.5 greenhouse gas scenario (O'Neill et al. 2016) was considered. Under this scenario, carbon dioxide concentrations would approximately double by 2100 (O'Neill et al. 2016, Fig. 3) and global mean temperature would increase by 2.7°C (uncertainty range 2.1–3.5 °C) relative to the pre-industrial era (IPCC 2021, Table SPM.1). The CORDEX simulations that downscale CMIP5 GCM runs were forced by an earlier version of this scenario, Representative Concentration Pathway RCP4.5. Depending on the model, the output data extend to 2099 or 2100.

Both the CORDEX and CMIP6 output data were interpolated onto a 0.125×0.125 degree grid covering Europe and the adjacent areas using bilinear interpolation. For the CORDEX data, interpolation effectively preserves the information, as the horizontal resolution of the original and interpolated data is similar, approximately 12 km. For CMIP6, we only examine the mean response of the 28 GCMs. The multi-GCM mean is very smooth (e.g., see Figs. 1a, c, S5a), and therefore interpolation does not result in significant loss of information. Still, if the present hybrid method is applied to the output of individual GCMs in the future, it may be necessary to employ a more sophisticated interpolation procedure for the GCM data prior to the actual analysis. To determine the climate change signal, 30-year means were calculated for each calendar month. Projected changes are expressed relative to the average of the 1981–2010 reference period.

Table 1 EURO-CORDEX model runs analysed: acronym and country of origin of the RCM, the driving CMIP5 GCM and the ordinal number of the realisation

	CORDEX model	Country	Driving GCM	Realisation
1	CNRM-ALADIN63_v2	France	CNRM-CM5	r1
2	CLMcom-CCLM4-8-17_v1	Germany	CNRM-CM5	r1
3	CLMcom-CCLM4-8-17_v1		EC-EARTH	r12
4	CLMcom-CCLM4-8-17_v1		HadGEM2-ES	r1
5	CLMcom-CCLM4-8-17_v1		MPI-ESM-LR	r1
6	DMI-HIRHAM5_v2	Denmark	EC-EARTH	r3
7	DMI-HIRHAM5_v2		HadGEM2-ES	r1
8	DMI-HIRHAM5_v3		NorESM1-M	r1
9	KNMI-RACMO22E_v2	Netherlands	CNRM-CM5	r1
10	KNMI-RACMO22E_v1		EC-EARTH	r1
11	KNMI-RACMO22E_v2		HadGEM2-ES	r1
12	GERICS-REMO2015_v1	Germany	NorESM1-M	r1

RCMs originate from the following organisations: CLMcom—Climate Limited-area Modelling Community; CNRM—Centre National de Recherches Météorologiques; DMI—Danish Meteorological Institute; GERICS—Helmholtz-Zentrum Geesthacht, Climate Service Center Germany; and KNMI—Royal Netherlands Meteorological Institute

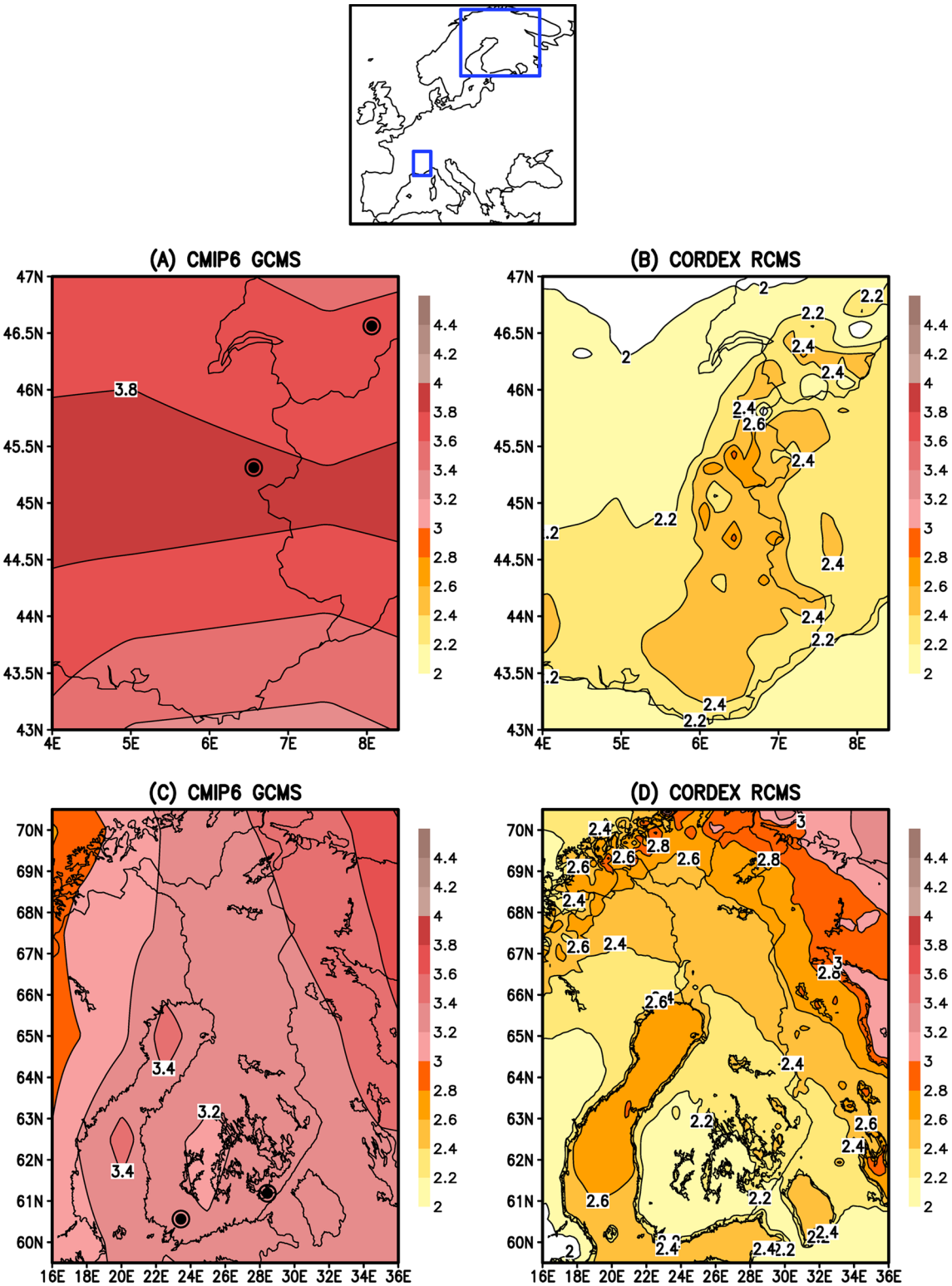

Fig. 1 Projected change in mean surface air temperature (in °C) in June-August from the period 1981–2010 to 2070–2099 over the western Alps: the averages of **a** 28 CMIP6 GCMs (under SSP2-4.5) and **b** 12 EURO-CORDEX RCM runs (RCP4.5). The model runs included are described in Sect. 2. Corresponding projections for Fennoscandia are given in **c** and **d**. In **a** and **c**, black dots indicate the four sample grid points considered later in this paper: (45.3125° N, 6.5625° E), (46.5625° N, 8.0625° E), (60.5625° N, 23.4375° E) and (61.1875° N, 28.4375° E). The positions of the sub-domains are shown in the European-wide map on the top

3 The GCM-RCM hybrid method

For the hybrid method, two variants of are introduced. The basic variant is particularly applicable when the temperatures of seas and inland water bodies are simulated in both RCMs and GCMs. The more complicated land–sea resolving variant may be preferred when reliable surface temperature data for water-covered areas are not available.

3.1 The basic variant

The philosophy behind the GCM-RCM hybrid method developed in this study is analogous to that of the widely used pattern-scaling technique. In pattern scaling, the local response of a climate variable to a different forcing scenario is calculated by multiplying the response produced by the existing simulation by the ratio of the simulated global mean temperature increases in the two scenarios (IPCC 2021, Section 4.2.4). In the present method, by contrast, scaling is applied to the responses produced by the two categories of climate models, GCMs and RCMs. Moreover, instead of the global mean temperature change, the spatial mean change over an area surrounding the target point is used for scaling:

$$\Delta X_{i,j} = \frac{\langle \Delta X^{GCM} \rangle}{\langle \Delta X^{RCM} \rangle} \Delta X^{RCM}_{i,j} \tag{1}$$

where ΔX represents the change of a climate quantity (e.g., near-surface air temperature) from the recent past (here 1981–2010) to future period (e.g., 2070–2099), (i, j) refers to the grid point under consideration, and the indices *GCM* and *RCM* stand for the multi-GCM and multi-RCM run averages. $\langle\ \rangle$ denotes the spatial mean over the area surrounding the point, calculated on the 0.125×0.125 degree grid for both model categories. By default, the mean is calculated over a square with a width of $\Delta\phi = 5°$ in the meridional direction and $\Delta\phi / \cos\phi$ in the zonal direction, or approximately 560×560 km (280 km from the grid point to each cardinal point). For a sensitivity study, experiments were also carried out with an averaging window half as narrow and twice as wide as the default (Sect. 4.3).

With a little algebra (1) can be converted into a mathematically equivalent form:

$$\Delta X_{i,j} = \langle \Delta X^{GCM} \rangle + \Delta X^{RCM}_{i,j} - \langle \Delta X^{RCM} \rangle + \frac{\langle \Delta X^{GCM} \rangle - \langle \Delta X^{RCM} \rangle}{\langle \Delta X^{RCM} \rangle} \left(\Delta X^{RCM}_{i,j} - \langle \Delta X^{RCM} \rangle \right)$$

By omitting the last non-linear term on the r.h.s., we obtain the alternative linearised version of the GCM-RCM hybrid method:

$$\Delta X_{i,j} = \langle \Delta X^{GCM} \rangle + \Delta X^{RCM}_{i,j} - \langle \Delta X^{RCM} \rangle \tag{2}$$

By examining Eqs. (1) and (2), it is readily seen that in both cases the regional mean of the change over the averaging square is identical to the corresponding change in the GCM simulations $\langle \Delta X^{GCM} \rangle$. Accordingly, both methods indeed introduce additional spatial details in the projection, but the regional mean of the change is still the same as that simulated by the GCMs. The window used to compute the spatial mean is allowed to move so that it is always located symmetrically around the target point.

Using the downscaling signal *DS* defined in Eq. (1) of Giorgi et al. (2016), (2) might simply be expressed in the form $\Delta X^{GCM}_{i,j} + DS$. Nonetheless, when calculating the spatial means, Giorgi et al. (2016) used a fixed area encompassing the Alps and nearby land areas instead of a moving window.

Equation (1) cannot be applied for precipitation since the spatial average of the change in the denominator can then come close to zero, making the division to explode. For precipitation, only the linear version (2) is thus usable. There are no such limitations for temperature, because when going far enough ahead into the future from the reference period, ΔT is unequivocally positive.

In the present analyses, ΔX^{GCM} in Eqs. (1) and (2) invariably represents the mean response of the 28 GCMs. For ΔX^{RCM} an average of the 12 runs listed in Table 1 is used, but to derive an uncertainty estimate, this technique is also applied independently to the individual RCM runs. In the calculation of averages over the CMIP6 (CORDEX) data, each model (model run) is assigned an equal weight. For both temperature and precipitation, the GCM-RCM hybrid projections are calculated in absolute units (°C or mm/day).

3.2 Alternative approach: the land–sea resolving variant

In many EURO-CORDEX simulations, the contrast in simulated near-surface air temperature change over sea and inland water regions compared to nearby continental areas is partly pre-determined. This is so because in those RCMs changes in the water surface temperature have been adopted from the driving GCM (Pietikäinen et al. 2018, and references therein). The imperfect treatment of aerosol forcing in the CORDEX RCMs results in a too weak warming over land, but has a smaller impact on the evolution of air temperatures over water-covered areas. Thus, the temperature changes over land and water become inconsistent with each other, and steep gradients in warming are generated along the coastlines.

To address this issue, we developed an alternative variant of the hybrid method that takes into account the distribution of land and water surfaces in the RCM simulation. In this variant, the area averages $\langle \Delta X^{GCM} \rangle$ and $\langle \Delta X^{RCM} \rangle$ used in

(1) are replaced by $\langle w\Delta X^{GCM}\rangle$ and $\langle w\Delta X^{RCM}\rangle$, where the weights are calculated by:

$$w_{i,j} = m_0 m_{i,j} + (1 - m_0)(1 - m_{i,j}) \quad (3)$$

where m_0 stands for the proportion of land area at the target point and $m_{i,j}$ at the point (i, j) in the surrounding area. In (3), both m_0 and $m_{i,j} \in [0, 1]$.

Accordingly, for a pure land point ($m_0 = 1$), the spatial mean over the 5×5 ° square is now calculated by omitting all grid cells consisting exclusively of water surface and giving a reduced weight to the mixed water-land cells. Correspondingly, for a water point ($m_0 = 0$) all completely continental points are disregarded. If the target grid point represents a combination of water and land ($0 < m_0 < 1$)), all the points within the square are included, but the weights depend on the fractions of land and water at both the target and the surrounding points. For example, if $m_0 \ll 1$, points dominated by water surface have a much higher weight than those dominated by land.

Here, the land–sea fractions used in (3) is the average of the fractions used in the five CORDEX RCMs analysed (Table 1). The differences among the RCMs in the land–water distributions are very small. In addition to the coastal areas, there are numerous mixed land–water grid cells in the Northern European lake-rich areas and the Greek archipelago, for instance (Fig. S1).

4 Results

4.1 Changes in temperature using the basic variant

We first examine summer temperature responses in two case study regions where dynamical downscaling has generated abundant small-scale details. In the Western Alps, orographic variations are large, while in Fennoscandia meandering coastlines and numerous inland water bodies create a complex distribution of land and water surfaces.

Figure 1b and d reveal that in the CORDEX RCM runs, warming is considerably amplified in the elevated regions of the Alps and over the seas and inland waters in Northern Europe. Conversely, in the the CMIP6 GCM simulations (Fig. 1a, c), the influence of the Alps is hardly discernible and, for example, there is only a minor increase in warming over the Gulf of Bothnia.

In the temperature projections produced by the GCM-RCM hybrid method, the overall level of warming is maintained similar to that simulated by the CMIP6 GCMs (Figs. 2, 3), but regional details originating from the CORDEX simulations, such as the stronger warming of the Alpine highlands, the bays of the Baltic Sea and Fennoscandian inland lakes, are apparent as well. Small-scale spatial variations in the temperature change fields are of the order of 1 °C at most in the Alps and somewhat smaller in Northern Europe (Fig. 3a, c). In the linearised version of the hybrid method (2), small-scale features are less pronounced than in the non-linear one (1). This can be understood by studying the non-linear term separating Eqs. (1) and (2). Since summer temperatures increase more strongly in the CMIP6 GCM than CORDEX RCM simulations, the first factor of the product is positive. Hence, the non-linear term is positive in those areas where RCM-simulated warming is stronger than in the surroundings (and vice versa). Thus, the non-linear term indeed tends to amplify regional details in the projected change.

Small-scale modifications generated by the hybrid method for the Alpine region (Fig. 2a–b) are qualitatively similar to those in Fig. 12e of Boé et al. (2023). A quantitative comparison is precluded by the different model ensembles and forcing scenarios applied in the studies.

Figure 4 provides the time series of the summer mean temperature change for two grid points in both example areas. At these points the modifying effect of the GCM-RCM hybrid method is opposite in sign.

Throughout the entire time series, warming is much weaker in the CORDEX RCM runs than in the CMIP6 GCMs (Fig. 4). The modifying impact of the hybrid methods is likewise consistent: in Fig. 4b and c the resulting warming is weaker than in the CMIP6 simulations, whereas the opposite is true in Figs. 4a and d. In the linearised version, deviations from the CMIP6 response are somewhat smaller than in the non-linear version.

Figure 5a illustrates the impact of differences among the CORDEX RCM runs on the GCM-RCM hybrid projection (the basic variant). Hybrid temperature responses corresponding to the various CORDEX runs diverge more pronouncedly in the Alps than in Northern Europe. At the southern point of the Alps (45.31° N, 6.56° E), all CORDEX runs, with the exception of one, lead to an intensification of warming compared to the CMIP6 multi-model mean. Thus, the inference that local hybrid warming is larger than the pure GCM estimate is robust. It should be noted that a single CORDEX run (run #10 in Table 1 or RACMO22 driven by EC-Earth) results in a considerably higher hybrid warming than the remaining ones.

At the northern Alpine point (46.56° N, 8.06° E), the GCM-RCM hybrid projection derived from the average of all CORDEX runs is about 0.5°C cooler than the CMIP6 projection (Fig. 4b). However, the modifications calculated from the individual CORDEX runs vary substantially (Fig. 5a), five RCM runs acting to increase and seven runs to decrease warming. Consequently, there is no real evidence about the direction of the impact.

In south-western inland of Finland (60.56° N, 23.44° E), the individual CORDEX runs quite unanimously

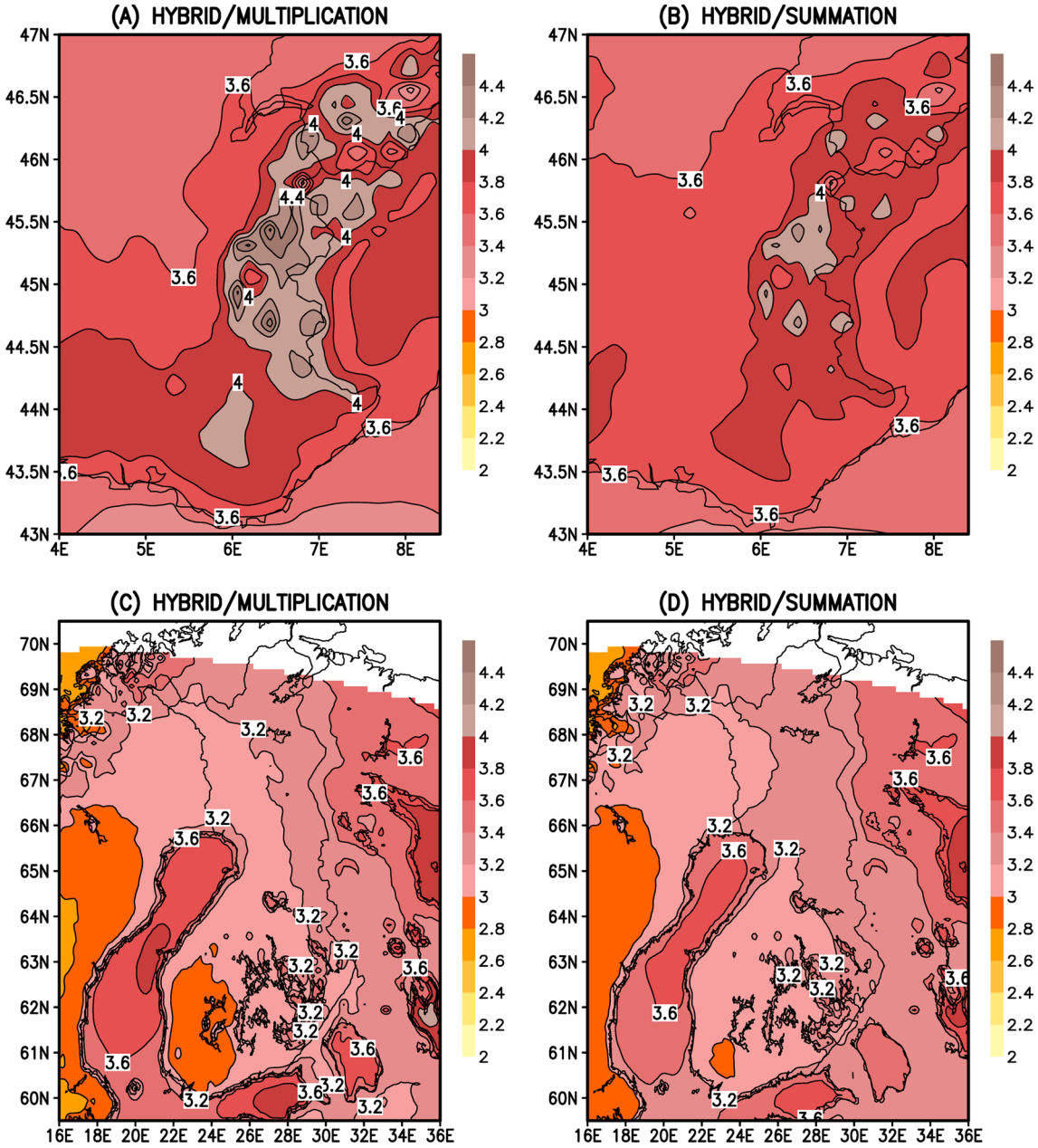

Fig. 2 Hybrid GCM-RCM temperature projection for June–August (in °C) from the period 1981–2010 to 2070–2099 under the SSP2-4.5 scenario over the western Alps produced by the basic variant with **a** the multiplication (Eq. (1)) and **b** summation method (Eq. (2)). Corresponding hybrid projections for Fennoscandia are shown in **c** and **d**

tend to weaken the warming (Fig. 5a), even if the modification calculated from the mean of the 12 runs is rather small, about −0.3 °C (Fig. 4c). At the eastern Finnish point (61.19° N, 28.44° E), located in the Saimaa lake district, the GCM-RCM hybrid temperature increase derived from the multi-RCM mean is only slightly stronger than the CMIP6 response, but 10 of the 12 RCM runs still act to intensify the warming.

As shown in the Appendix of this paper, in the Western Alpine case study region, for instance, also the original temperature responses produced by the individual CORDEX RCM runs differ substantially from one another. For example, RACMO22 exhibits much more variability at the grid-point scale than CCLM4. Using Eqs. (1) or (2), such spatial variations are immediately transferred to the GCM-RCM hybrid projection. Roughly it can be said that the general level of enhanced warming in the Alpine region (Fig. 2a) is substantially contributed by the CCLM4 model, while small-scale details in the temperature response are predominantly induced by RACMO22 and HIRHAM5.

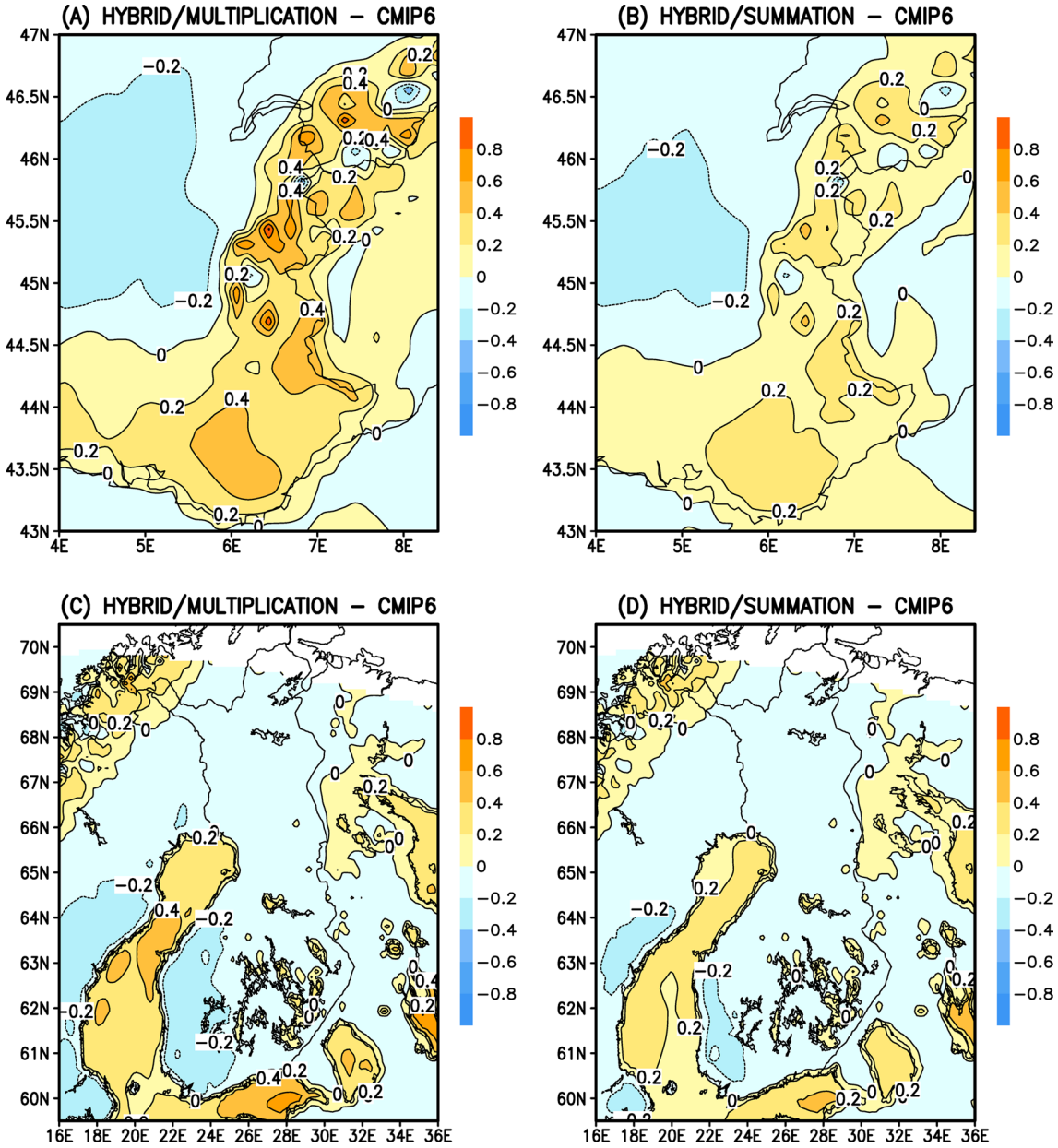

Fig. 3 Differences between GCM-RCM hybrid (basic variant) and CMIP6-simulated June-August temperature responses (in °C) from 1981–2010 to 2070–2099 under SSP2-4.5 over the western Alps and Fennoscandia: **a**, **c** projections obtained by multiplication (Eq. (1)) minus the 28-GCM mean and **b**, **d** response by summation (Eq. (2)) minus the GCM mean. Thus, each panel shows the difference between the corresponding panel in Fig. 2 and **a** or **c** of Fig. 1

Figure 6 shows the geographical distribution of the temperature change modification produced by the basic variant of the GCM-RCM hybrid method compared to the GCM response for the entire European area in all four seasons, while inter-RCM agreement is considered in Fig. 7. In summer, the consensus of the CORDEX runs regarding the sign of the modification is good (10–12 runs yield modifications with like signs) in large areas of Western and Northern Europe, for example, over the Baltic Sea and its adjacent areas, and also in a portion of the Alps. However, at those Alpine grid points where the hybrid method tends to reduce the change compared to the multi-GCM mean response, the agreement is invariably rather low. In the other seasons, the signal is generally less robust and predominantly found in Southern Europe.

Also, the magnitude of the impact is generally largest in summer, when the hybrid method intensifies warming over the Baltic Sea, the Scandinavian mountain range and the Alps and on the Mediterranean coasts. Conversely, weakening is seen over the Western Mediterranean Sea

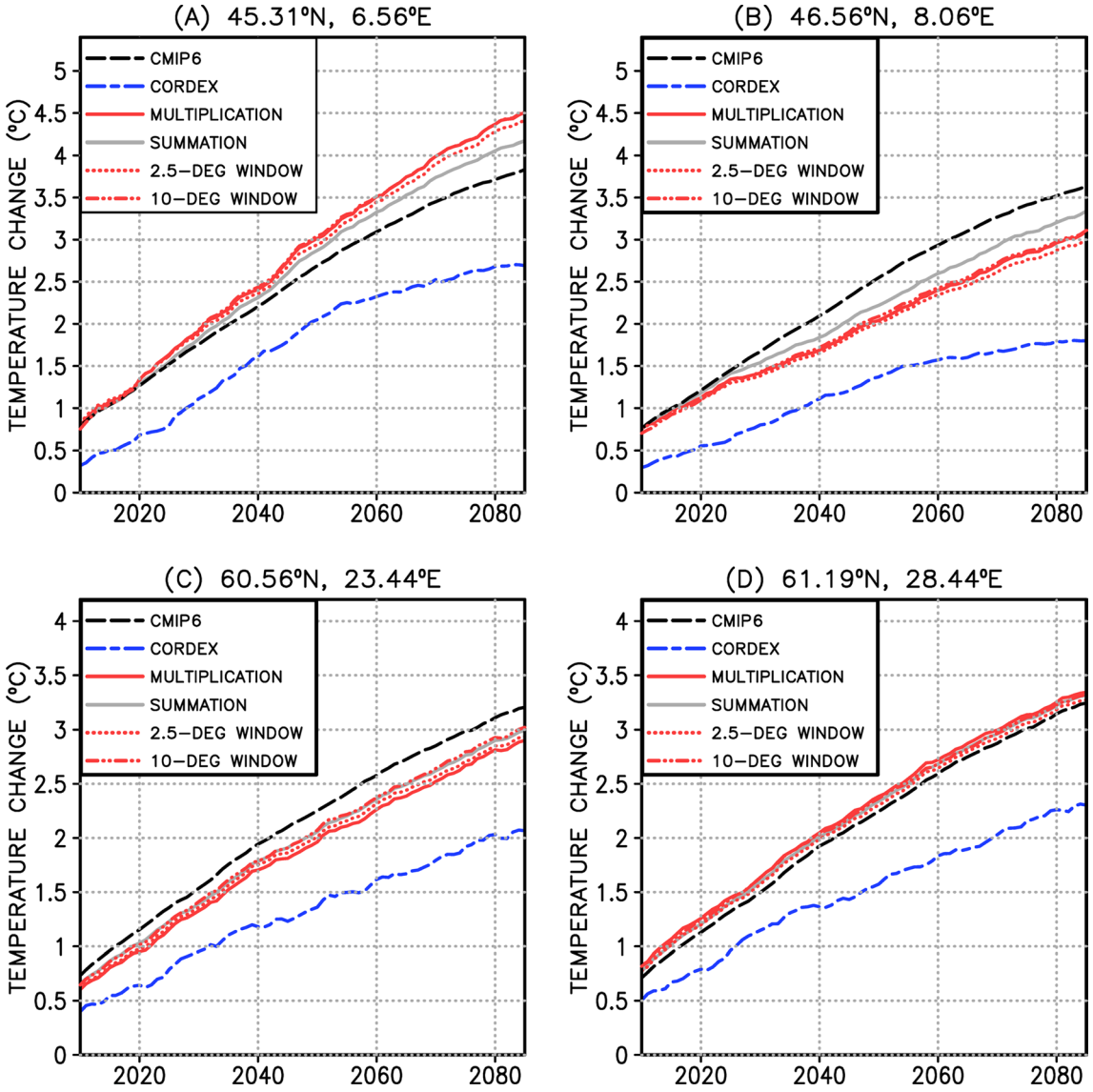

Fig. 4 30-year running mean temperature changes in June–August (in °C) relative to the period 1981–2010 during the 21th century at the four grid points shown in Fig. 1: **a** 45.31° N, 6.56° E, **b** 46.56° N, 8.06° E, **c** 60.56° N, 23.44° E and **d** 61.19° N, 28.44° E. Denotations in the legend: CMIP6—28-GCM mean; CORDEX—mean of the 12 EURO-CORDEX runs; MULTIPLICATION—hybrid GCM-RCM response produced by multiplication (1); SUMMATION—hybrid GCM-RCM response produced by summation (2); 2.5-DEG/10-DEG WINDOW—hybrid responses calculated by the multiplication technique using 2.5 and 10° windows for spatial averaging

and in land areas bordering the Baltic Sea (Fig. 6). On the other hand, in most parts of Central and Eastern Europe, the effect of modification is weaker than ±0.2 °C in all seasons, indicating that the original CMIP6-simulated temperature response remains largely unchanged. The response created by the GCM-RCM hybrid method suffers nowhere in Europe from the systematic underestimation of large-scale warming that is characteristic for the current CORDEX runs. In large areas of Central and Eastern Europe, the hybrid temperature increase in summer was found to be 1.5–2 °C larger than the average warming in the presently-analysed CORDEX simulations.

An interesting question is why RCMs tend to simulate the most pronounced spatial variability for the most of Europe especially in summer. Presumably, one reason for this is the weak basic flow in the atmosphere, which reduces the impact of advection in comparison to other seasons. Moreover, solar radiation is most intense in summer, and consequently the influence of various feedback mechanisms related to radiation are at their strongest.

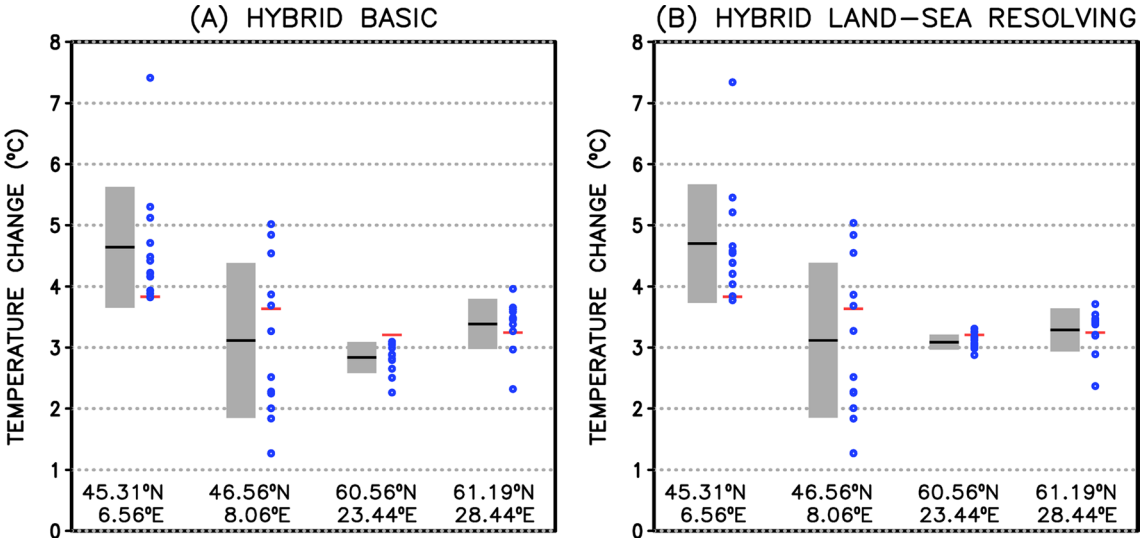

Fig. 5 Uncertainty induced by inter-RCM differences in the GCM-RCM hybrid temperature change (the multiplication approach, unit °C) in June-August from 1981–2010 to 2070–2099 under SSP2-4.5 at the four points considered in Fig. 4: **a** the basic variant **b** the land–sea resolving variant. Blue dots: hybrid temperature projections calculated using the individual EURO-CORDEX runs listed in Table 1; red lines: the 28 CMIP6 mean changes; grey bars with a black line: the mean ± standard deviation of the hybrid temperature change estimates derived from the individual CORDEX runs

4.2 Changes in precipitation: the basic variant

In most parts of Europe, the modifications of precipitation change generated by the GCM-RCM hybrid method using the individual CORDEX runs diverge even in sign (Fig. 9). Nonetheless, some degree of signal can be seen in the Baltic Sea region in autumn and winter. In particular, over the Southern Baltic Sea the use of the hybrid method leads to a slight increase in precipitation during these seasons (Fig. 8). To provide another example, the incorporation of RCM data tends to increase precipitation over the Adriatic Sea in summer and reduce it in surrounding land areas.

In the Alps, the precipitation projection produced by the hybrid method was found to follow the multi-CORDEX mean response rather than the CMIP6 response. This is due to the fact that absolute precipitation changes simulated by the CMIP6 GCMs are, on average, much weaker than grid-point scale changes simulated by the CORDEX runs (Fig. S5). A trivial reason for this is that the baseline precipitation is much larger in elevated than lowland areas, a feature that is only properly resolved by RCM simulations (e.g., Torma et al. 2015, Fig. 4). In low-lying areas, absolute precipitation changes are much more modest than over mountain ranges and are of the same order of magnitude in both model categories (Fig. S5). It should be noted that the present 12-RCM mean precipitation response is mostly negative even in the elevated areas of the Alps (Fig. S5), in contrast to Torma et al. (2015) and Giorgi et al. (2016). This discrepancy may be attributed to the different RCM ensemble and forcing scenario studied, given that the inter-RCM agreement on precipitation changes is low (Fig. 9).

In the the Scandinavian mountain range region, the influence of the GCM-RCM hybrid method on precipitation response is opposite in autumn (intensification on the western slopes) and in winter (intensification on the eastern slopes). Owing to the better resolution of orography, these features presumably reflect the stronger influence of mountain ranges on local precipitation in RCMs than in GCMs. For example, in autumn the westerly component of the geostrophic wind was found to strengthen in three of the five CMIP5 GCMs providing boundary data (Table 1). This leads to an increase in orographic precipitation on the western side of the Scandinavian mountains and a decrease on the eastern side, and this change is better resolved in RCMs than GCMs. A quantitative investigation of this issue is left as a topic for future research.

4.3 Sensitivity to the width of averaging window

The impact of the window size used for spatial averaging in (1) is outlined in Fig. S2. In order to identify small-scale details, the temperature responses themselves are only shown for the Western Alps region. Conversely, the difference fields are given for the whole of Europe.

At the smallest spatial scales, the temperature response calculated with the GCM-RCM hybrid method is fairly independent of the size of the averaging window; the patterns shown in Figs. 2a (window length of 560 km) and S2a, b (280 and 1120 km) are very similar. The

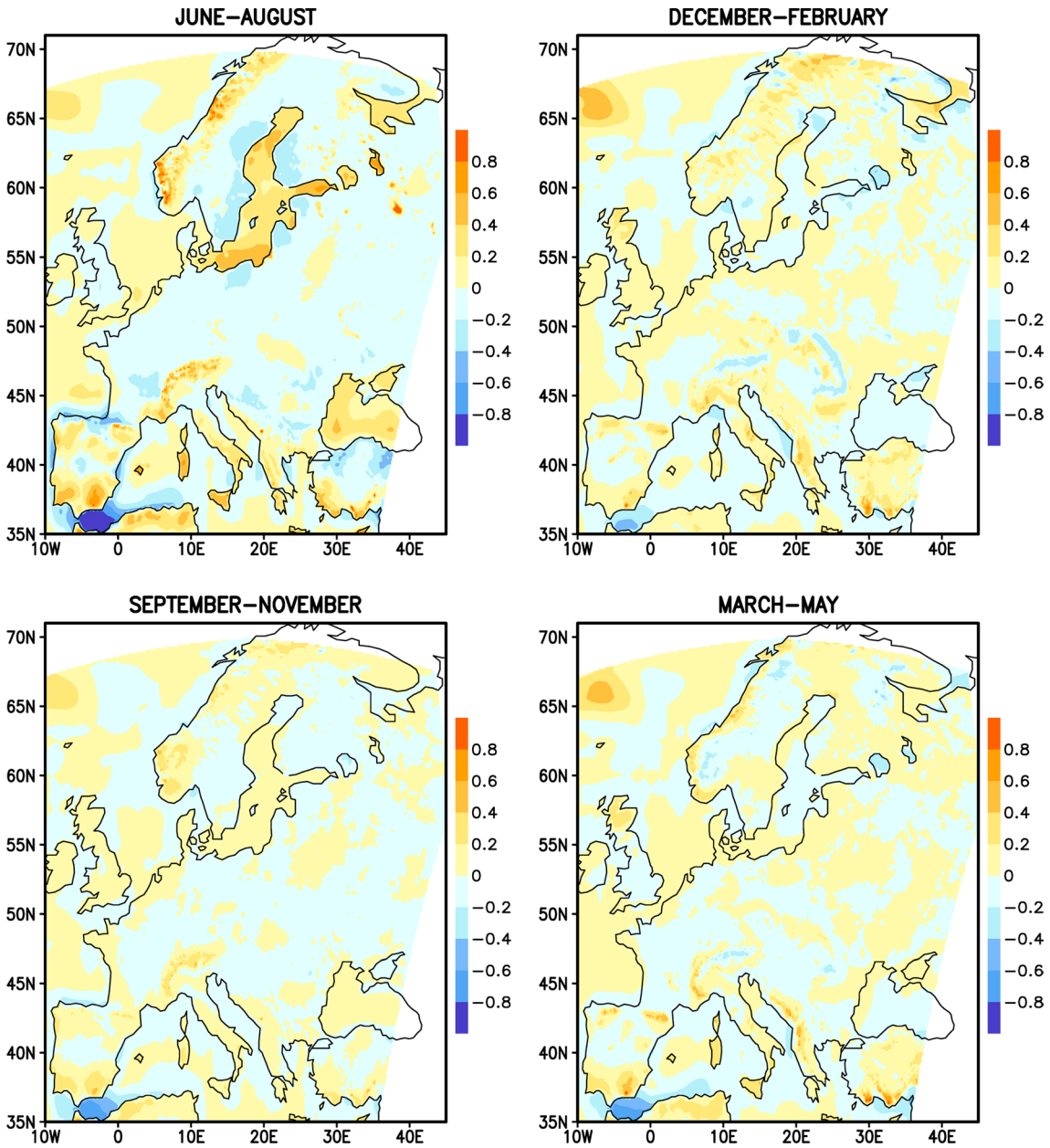

Fig. 6 Differences between the GCM-RCM hybrid (produced by the basic variant with multiplication, Eq. (1)) and 28-GCM mean seasonal temperature responses from 1981–2010 to 2070–2099 under SSP2-4.5 in June–August (upper left), September–November (lower left), December–February (upper right) and March–May (lower right). Unit °C

inter-window size differences are mainly ~ 0.2 °C or smaller (Fig. S2c–d). The validity of this finding for the entire time series from the 2010s to 2080s at the four example points is illustrated in Fig. 4. Accordingly, the overall conclusion regarding where and how much the hybrid method strengthens or weakens the warming compared to the CMIP6 response is not very sensitive to the selection of the window size. Furthermore, the choice of window size has the most pronounced impact at the horizontal scales of 200–1000 km rather than at the grid point level. This is so because the scaling factor $\langle \Delta T^{GCM} \rangle / \langle \Delta T^{RCM} \rangle$ in (1) is nearly identical at two adjacent points, as 95–98.75% of the grid points over which the spatial mean is calculated are the same.

In CMIP6 GCMs, the nominal horizontal resolution is typically 100–200 km. This is the absolutely smallest spatial scale that can be simulated for parameterized physical phenomena, e.g., the impact of surface albedo on shortwave radiation balance. Nevertheless, the effective resolution, or the scale at which the shape of the kinetic

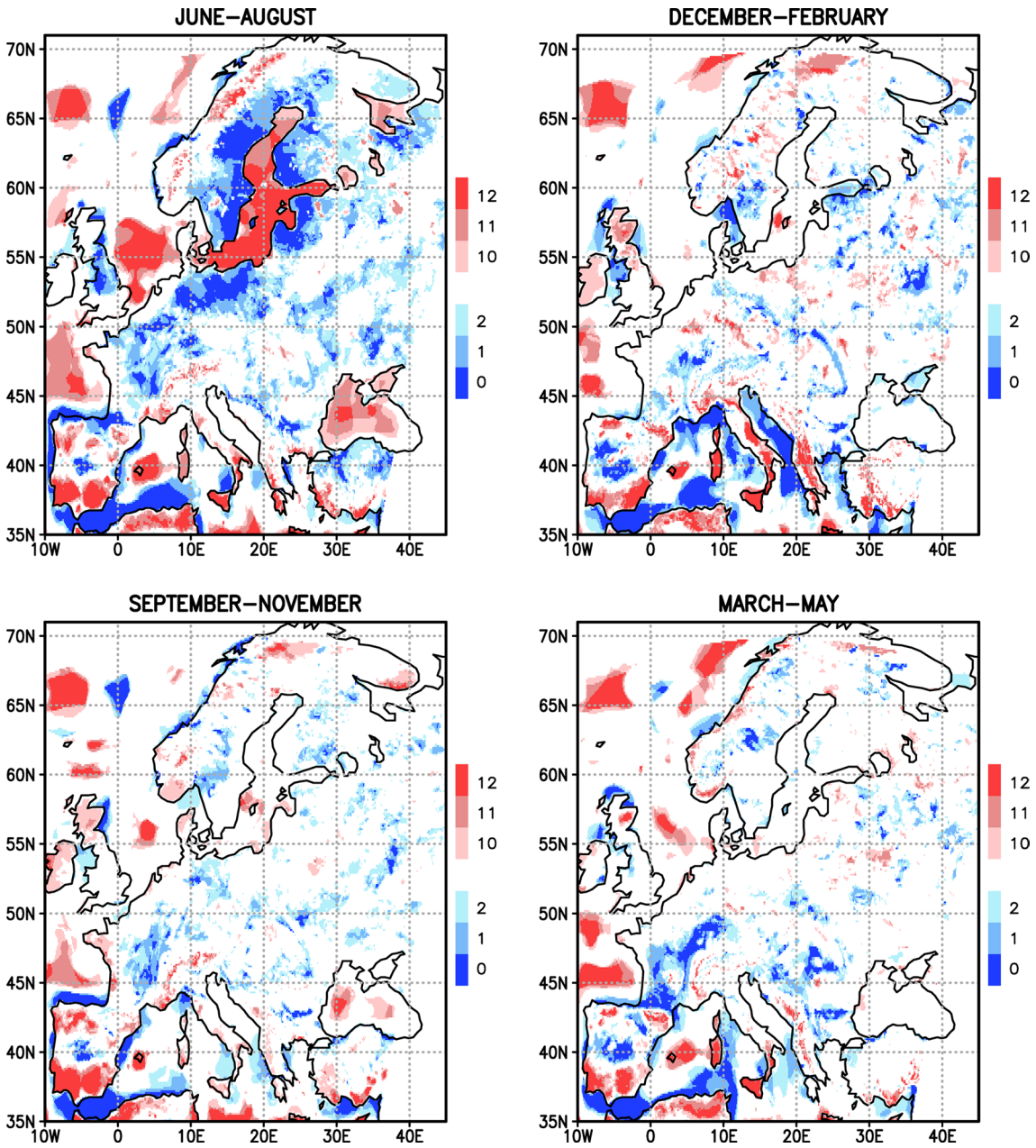

Fig. 7 The number of CORDEX RCM runs the use of which leads to a strengthening of the seasonal mean temperature increase compared to the 28-GCM mean response in the calculation of the GCM-RCM hybrid temperature response (basic variant) for the period 2070–2099 under SSP2-4.5. As indicated by the colour bars, in the areas with reddish (bluish) shading 10–12 (0–2) out of the 12 CORDEX runs act to intensify the temperature increase

energy spectrum is correctly simulated, is about 3–5 times as large (Klaver et al. 2020). Hence, the finest horizontal scale of atmospheric dynamics that is represented properly in GCMs varies between about 300 km and 1000 km. The 560 km window width fits well within this range, while the 280 km (1120 km) window would fall slightly below the lower (above the upper) bound. Moreover, the wider the window, the broader the zone that is cut off at the edges of the domain. Accordingly, the 560 km window length appears to be a reasonable compromise.

4.4 Hybrid projections with the land–sea resolving variant

In this section, we focus on temperature projections, since near-surface air temperature is the variable that is most

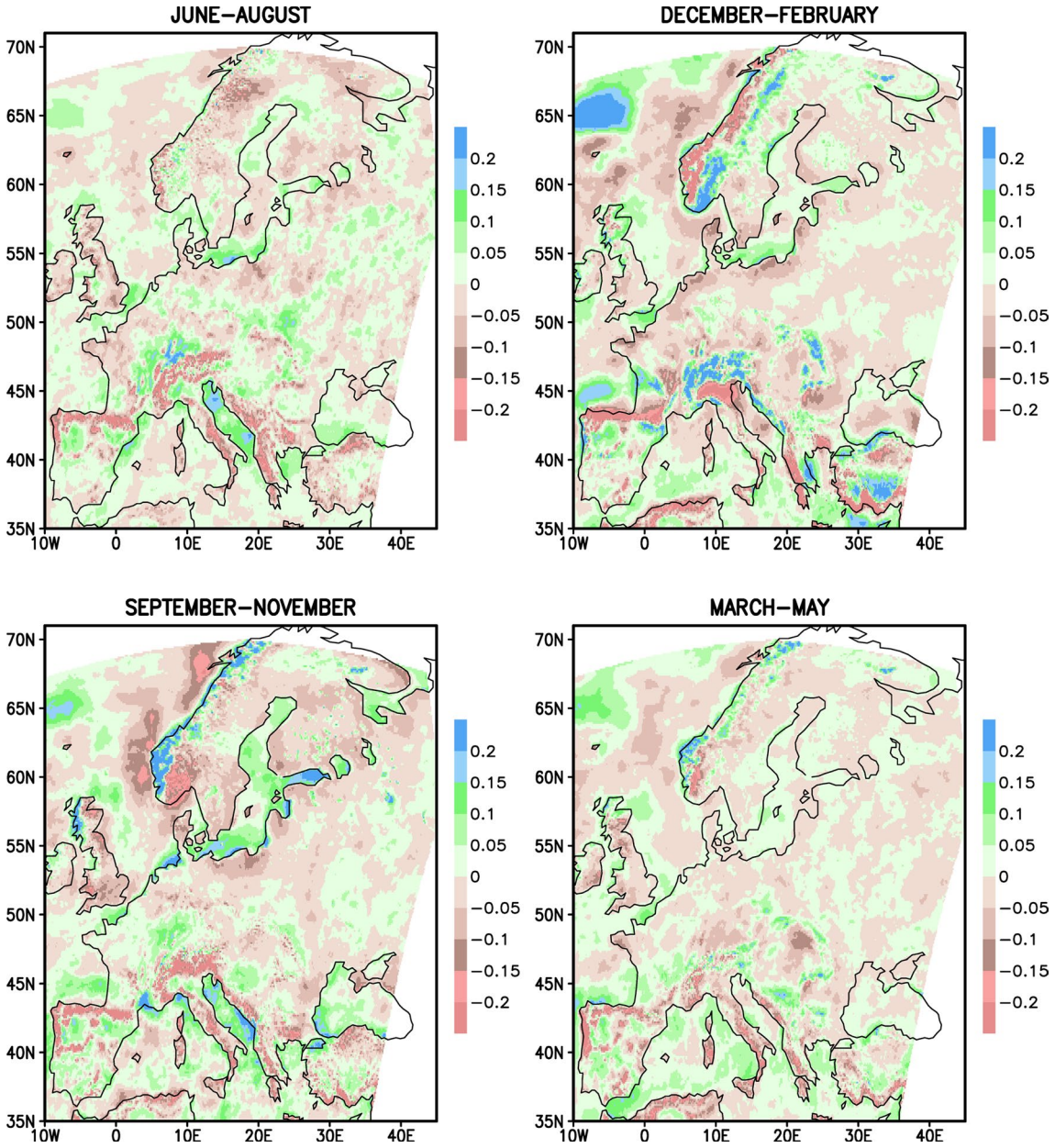

Fig. 8 Differences between the GCM-RCM hybrid (by the basic variant with summation, Eq. (2)) and 28-GCM mean seasonal precipitation responses from 1981–2010 to 2070–2099. Unit mm day^{-1}. For further information, see the caption of Fig. 6

directly related to the temperature of the underlying surface. Moreover, it was shown in Sect. 4.2 that the hybrid projections for precipitation are less robust than those for temperature.

We first examine the two example regions in summer. Over the Western Alps, the basic (Fig. 2a) and land–sea resolving (Fig. 10a) variants produce nearly identical projections, with differences only in the order of a few hundredths of a degree (Fig. 11, top-left panel). This is not unexpected since the fraction of water surface in this region is small, apart from the Mediterranean coast (Fig. S1). Moreover, the ratio of the CMIP6 to CORDEX-projected warming is fairly similar on both sides of the coast, so that the ratio $\langle \Delta T^{GCM} \rangle / \langle \Delta T^{RCM} \rangle$ in (1) does not depend significantly on whether the spatial averages are calculated by including both the sea and land areas or excluding either of them.

In contrast, for the Northern European sub-region in summer, the temperature responses in the basic (Fig. 2c) and land–sea resolving (Fig. 10b) variants differ by up to several tenths of a degree (Fig. 11). Furthermore, the differences from the CMIP6 response are smaller for the land–sea resolving variant (Fig. S3b) than the basic variant

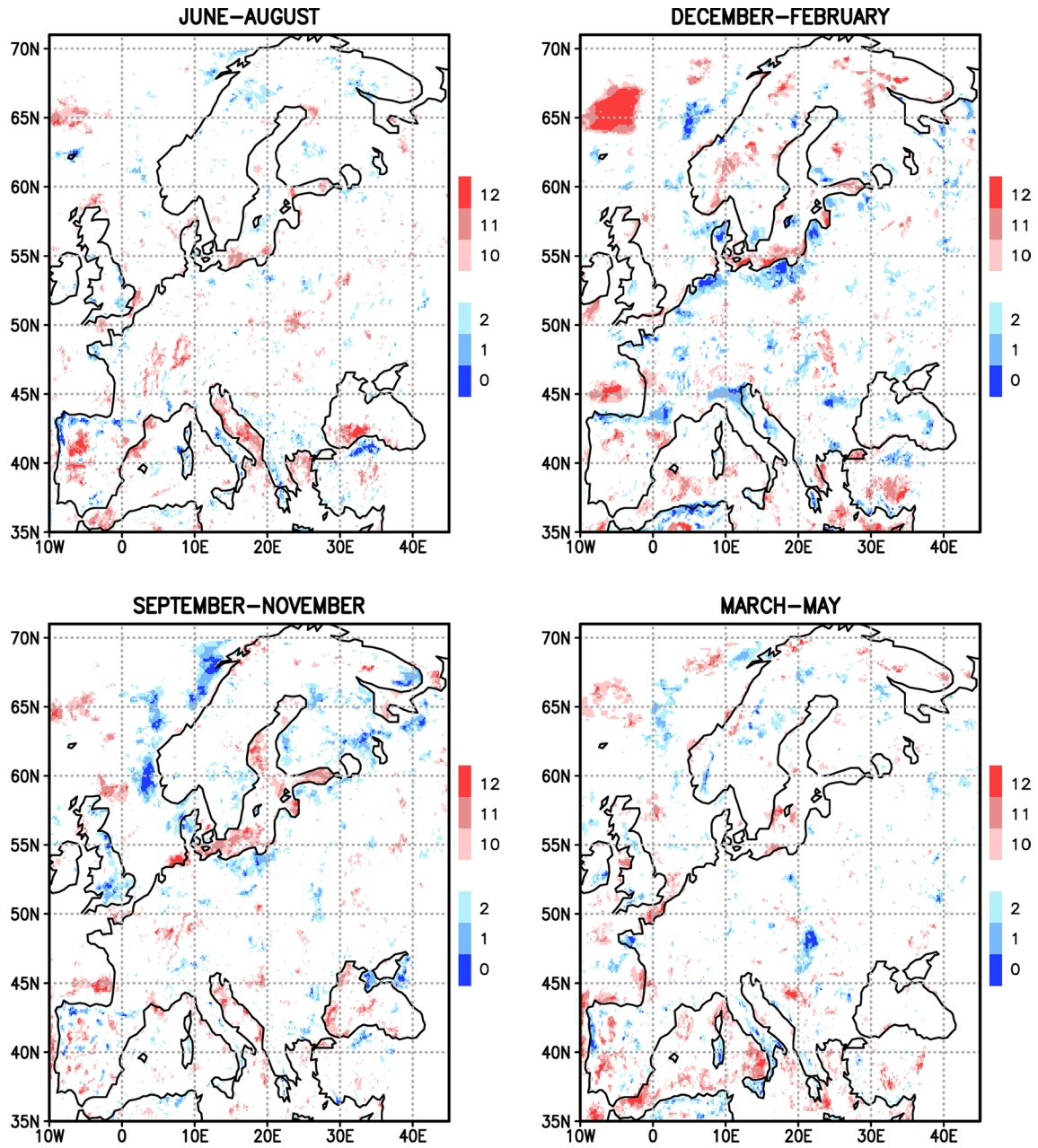

Fig. 9 The number of CORDEX RCM runs that produce a more positive GCM-RCM hybrid seasonal mean precipitation response compared to the 28-GCM mean. For further information, see the caption of Fig. 7

(Fig. 3c). In both cases the resulting warming over the lake districts and the Baltic Sea is stronger than over the adjacent continental areas, but in the land–sea resolving variant the differences are only about a half of those in the basic variant. In this region, in the CMIP6 GCMs warming is only ~ 0.2 °C larger over the sea than over the surrounding land areas (Fig. 1c), whereas in the CORDEX simulations the difference is about 0.7 °C (Fig. 1d). In addition, the Northern European sample area consists of a mixture of land and water-dominated grid cells. Therefore, the ratio $\langle \Delta T^{GCM} \rangle / \langle \Delta T^{RCM} \rangle$ is quite different depending on whether all grid points within the $5 \times 5^{\circ}$ square are included or only those that have a similar underlying surface to the target point.

Looking at the method-related differences for the whole of Europe, we see that in inland areas the hybrid responses produced by both variants are virtually identical (Figs. 11 and S4). This is true for most of the major European mountain ranges, such as the Alps, Pyrenees and

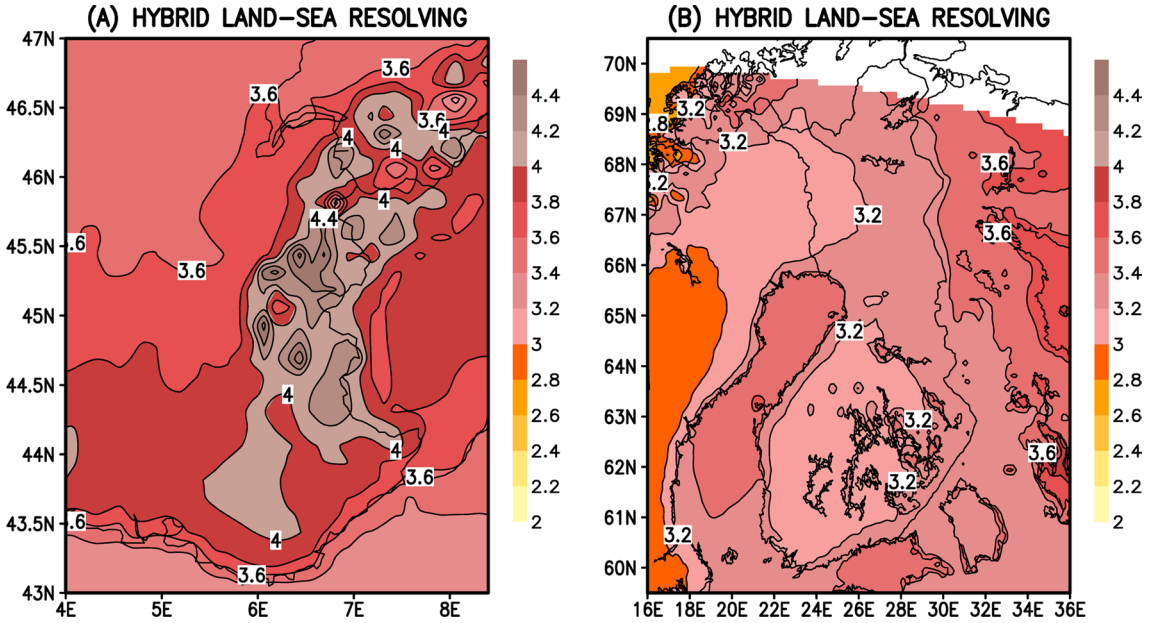

Fig. 10 Hybrid GCM-RCM temperature projection for June-August (in °C) from the period 1981–2010 to 2070–2099 under SSP2−4.5 over **a** the western Alps and **b** Fennoscandia produced by the land–sea resolving variant

Carpathians. The largest differences in projected warming, up to 0.2–0.3 °C, occur in some coastal areas, with the sign of the difference reversed across the coastline. Nevertheless, the fraction of the area with a non-negligible difference between the methods, > 0.1 °C, is fairly small. The largest differences occur in areas near the Baltic Sea in summer and the westernmost Mediterranean in all seasons.

Over the Western Alps region, the scatter of the hybrid projections derived from the individual CORDEX runs does not depend on the variant of the hybrid method either (Fig. 5a, b). For the Northern European sample points, the inter-RCM differences are much smaller when applying the land–sea resolving than the basic variant. In this area, which consists of a labyrinth of sea, continent, lakes and archipelago (Fig. S1), a large fraction of points within the $5 \times 5°$ averaging box are either not used at all or have a low weight when applying the land–sea resolving variant. Effectively, the land–sea resolving variant has a similar impact to reducing the size of the averaging square in (1). This inherently forces the ratio $\Delta T_{i,j}^{RCM} / \langle \Delta T^{RCM} \rangle$ to be closer to unity, thus reducing the impact of the RCM simulations on the outcome of the hybrid algorithm. We consider this to be a significant drawback of the land–sea resolving variant of the hybrid method.

5 Discussion

The GCM-RCM hybrid method proved to be more robust for near-surface air temperature than for precipitation (Figs. 7, 9). In most of Europe, local small-scale details in the precipitation change simulated by the different CORDEX runs diverge even in sign. An important factor behind this discrepancy is the substantial impact of natural variability on precipitation totals. Should the signal-to-noise ratio be higher, the hybrid method might also be better suited for treating precipitation responses.

When the individual CORDEX runs are examined separately, in some cases the resulting hybrid temperature projections likewise diverge substantially (Fig. 5). This is due to the fact that the CORDEX runs already simulate rather different temperature responses, examples of which are given in the Appendix. Future users of the method can themselves decide which RCM runs they regard as most plausible for simulating small-scale variations and only use those runs in preparing the hybrid projections. In this work, our primary goal was to introduce the method rather than publish any final climate change scenarios, and consequently, no very rigorous selection of the RCM runs was made.

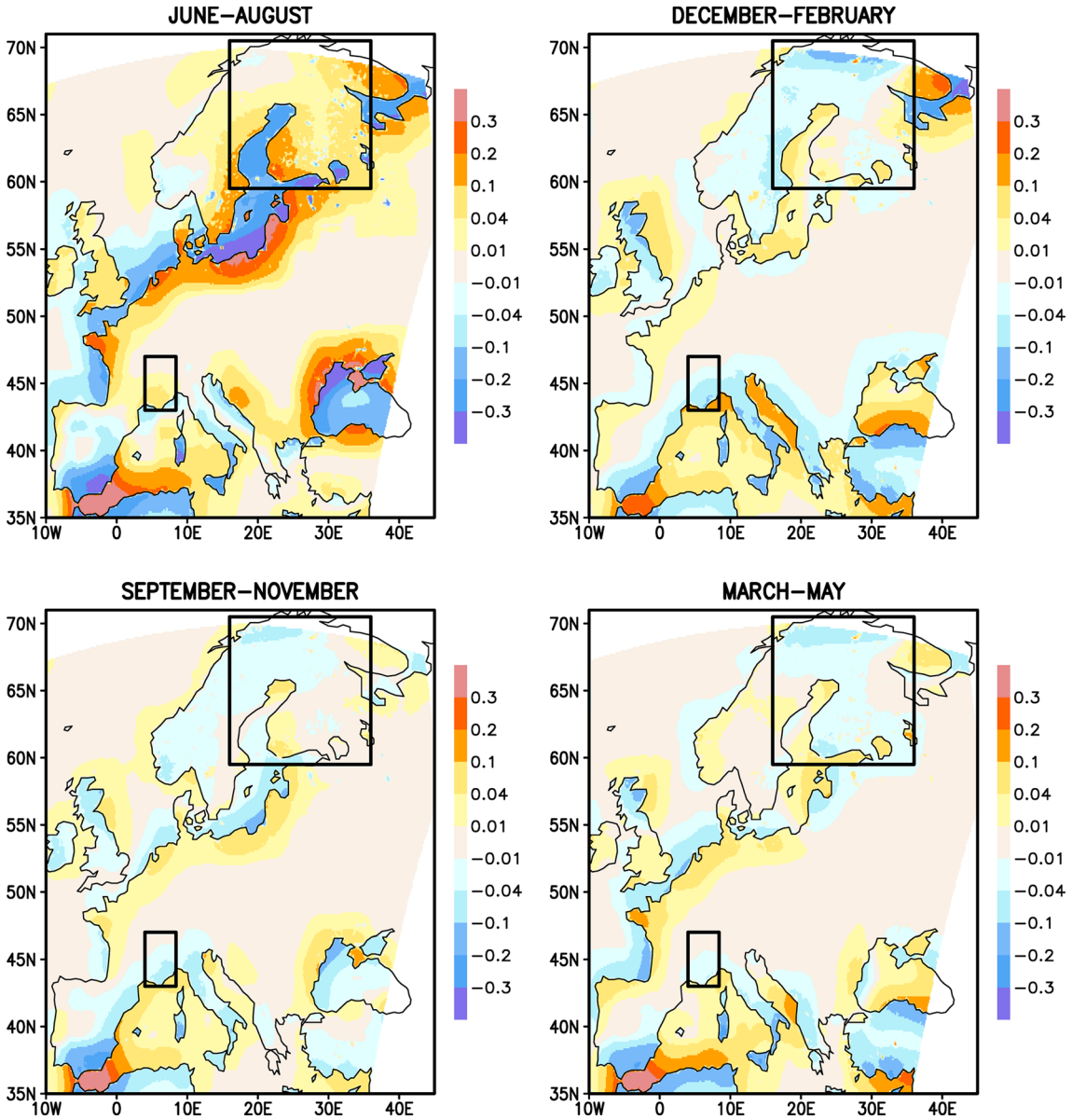

Fig. 11 Differences between the seasonal GCM-RCM hybrid temperature responses (from 1981–2010 to 2070–2099 under SSP2-4.5, unit °C) produced by the land–sea resolving and basic variant. Note the nonlinear colour scale. The Western Alpine and Fennoscandian subdomains are indicated by black rectangles

It is plausible that RCMs can simulate the impact of orographic variations (e.g., Figs. 1b, 2a) in a physically reasonable way, at least in a qualitative sense. In particular, the loss of snow cover tends to amplify warming in elevated areas through the surface albedo feedback (Giorgi 2019, p. 5704). Both variants of the hybrid method yielded virtually identical temperature projections for the main European mountain regions (Fig. 11). Conversely, for RCMs with a fixed change in sea surface temperature, the basic variant may overestimate gradients in the warming signal in coastal areas (Sect. 3.2). Certainly, it has long been recognised that even in such RCM experiments that include an interactive dynamical sea model, the projected warming over the Baltic Sea in summer tends to be stronger than over the surrounding land areas (Räisänen et al. 2004, Fig. 5). In the future, the basic variant of the method is likely to be the preferable approach if increasingly numerous RCMs include dynamic sub-models for the sea and water bodies. Prior to that, the alternative land–sea resolving variant may be more physically justified for RCMs employing pre-specified water surface temperatures. However, it is important to note that the land–sea resolving variant potentially underestimates the scatter induced by inter-RCM differences (Sect. 4.4).

We would like to stress that in the present study we do not want to devalue regional models in general nor the subset of EURO-CORDEX RCM runs investigated in this work. On the contrary, the present findings indicate that even if GCMs are primarily relied upon when considering large-scale climate change, RCM runs can provide valuable additional information on small-scale details, especially on the dependence of warming on orographic variations. Moreover, there are many meteorological phenomena, such as extreme precipitation events, for which usable information can only be obtained from fine-grid models (Jacob et al. 2014; Torma et al. 2015).

6 Conclusions

Using either GCM or RCM simulations alone is not an optimal way to produce regionally detailed climate change projections. GCMs are unable to resolve small-scale details in the climate response (Fig. 1), while RCM ensembles suffer from lack of adequate representativeness. Moreover, the currently available EURO-CORDEX runs have been shown to considerably underestimate warming, especially in summer.

The GCM-RCM hybrid method developed in this work exploits the benefits of both categories of models. The procedure is straightforward and can be easily programmed. The output data of GCMs and RCMs are only needed at the monthly mean level, which reduces the size of the files by a factor of ~30 compared to approaches requiring daily data, such as the downscaling method introduced by Boé et al. (2023). Both the GCM and RCM data should be interpolated onto the same dense grid, and the domain has to encompass, in addition to the area of interest, an edge half the width of the averaging window, or 280 km using the present default window length. The method can be readily applied to the output of those GCMs for which RCM downscalings are not available; the non-linear version even for a different greenhouse gas scenario. In this study, the method is exemplified by combining the latest generation CMIP6 GCM simulations with EURO-CORDEX RCM downscalings for the previous CMIP5 generation.

The philosophy of the GCM-RCM hybrid approach is akin to that behind the nudging technique, which relaxes large-scale features in the RCM run to approximate the driving GCM during the simulation across the entire domain. To achieve this, an adjustment term is inserted into the prognostic equations of the RCM, acting to reduce differences between the RCM and GCM runs (von Storch et al. 2000; Liu et al. 2012). Here, however, we are working with the output files of finished model runs, and therefore in the GCM-RCM hybrid method "nudging" is only executed afterwards.

Two versions of the hybrid method have been developed, of which only the linear version (2) is applicable for precipitation. For temperature projections, by contrast, non-linear scaling (1) may be more appropriate than the linear approach. This implicitly includes the pattern-scaling assumption that small-scale geographical variations in warming should be proportional to the area-averaged temperature increase (Sect. 3.1). In the basic variant, the spatial averages used for scaling are calculated over all the grid boxes within the $5 \times 5^\circ$ square surrounding the point (Sect. 3.1). In addition, we developed an alternative approach, the land–sea resolving variant (Sect. 3.2), which can be used if the surface temperatures of seas and inland watersheds are predefined in the RCM simulations.

To provide an example of a potential practical application, the current spatially detailed temperature projections that are free from the general RCM-simulated underestimation (Figs. 2, 10) are likely to be better suited for simulating snow melt and ablation of glaciers in mountain ranges than projections derived solely from either the GCM or EURO-CORDEX RCM output data (Fig. 1). Cryospheric simulations require temperature data representing the future climate at high temporal resolution. Such data can be derived, for example, by using the delta-change approach, that is, by adding the spatially fine-scale time-mean temperature response to historical daily or hourly temperatures extracted from observations or reanalyses. The resulting surrogate temperature data could also be used to project the length and degree days of future thermal growing seasons, with implications for phytogeographical regions and the conditions of agriculture. Even rough estimates of extreme temperatures might be feasible, depending on whether there will be significant changes in the standard deviation and higher moments of the frequency distribution of temperatures. Furthermore, the monthly mean temperature and precipitation projections produced by the hybrid method in themselves provide sufficient information to assess future changes in the Köppen climate zones (e.g., Cui et al. 2021) at high spatial resolution.

There is evidence that some CMIP6 GCMs overestimate the future global mean warming (e.g., Stolpe et al. 2021). In the latest IPCC assessment (IPCC 2021), projections of future global mean temperature change therefore incorporated observational constraints on past warming and the estimated equilibrium and transient sensitivity of the climate system. This resulted in a slight reduction in the projected warming compared to the direct use of climate model output, with the largest change at the upper end of the uncertainty range. Yet, such an overestimation of the model-simulated warming does not necessarily occur everywhere in the world. For example, Boé et al. (2020b) found that the previous-generation CMIP5 models tended to underestimate the observed summer warming in Western Europe but overestimated it in Eastern Europe. Conversely, the projected summer warming is on the average larger in CMIP6 than in CMIP5 models,

especially in Central and Southern Europe (Palmer et al. 2021). It is therefore an important topic for future research whether observationally constrained estimates of projected warming can also be meaningfully derived at sub-continental scales. Such estimates could be used as the basis for the GCM-RCM hybrid projections instead of the raw GCM output data. This may further improve the reliability of the resulting local temperature projections.

The problems identified in the EURO-CORDEX ensemble, i.e., the inadequate treatment of aerosol forcing and other key climate processes, will be hopefully alleviated in future generations of RCM simulations. Nevertheless, the representativeness of the RCM ensembles continues to be a concern, as computationally demanding RCM downscalings can only be executed for a fraction of all GCM simulations. This particularly concerns Convection Permitting Models that are very laborious. Employing the GCM-RCM hybrid method introduced in the present work, the matrix of fine-scale climate scenarios can be replenished by constructing regionally detailed surrogate projections for those GCMs for which RCM downscalings are wholly or partially missing.

Appendix

Figure 12 shows the temperature responses for summer in five individual CORDEX simulations. In all examples, both the RCM and the driving GCM are different.

It can be seen that the RACMO22 RCM produces very intense small-scale variations in the pattern of warming. The same proved to hold true for the other two runs of this model (Table 1). HIRHAM5 likewise simulates quite large variations at the grid-point scale. Conversely, for CCLM4 the temperature change field is fairly even. Such differences in the structure of the response are caused by the CORDEX models rather than the driving GCMs, as these features are repeated in a qualitative sense in all simulations of each individual RCM.

Such a very large inter-RCM divergence in regional variability evidently indicates that the local patterns of warming must be unrealistic in at least some of the models. Nonetheless, in this study we have not attempted to judge which of the CORDEX RCMs examined might be best in this respect. In any case, discrepancies among the different runs

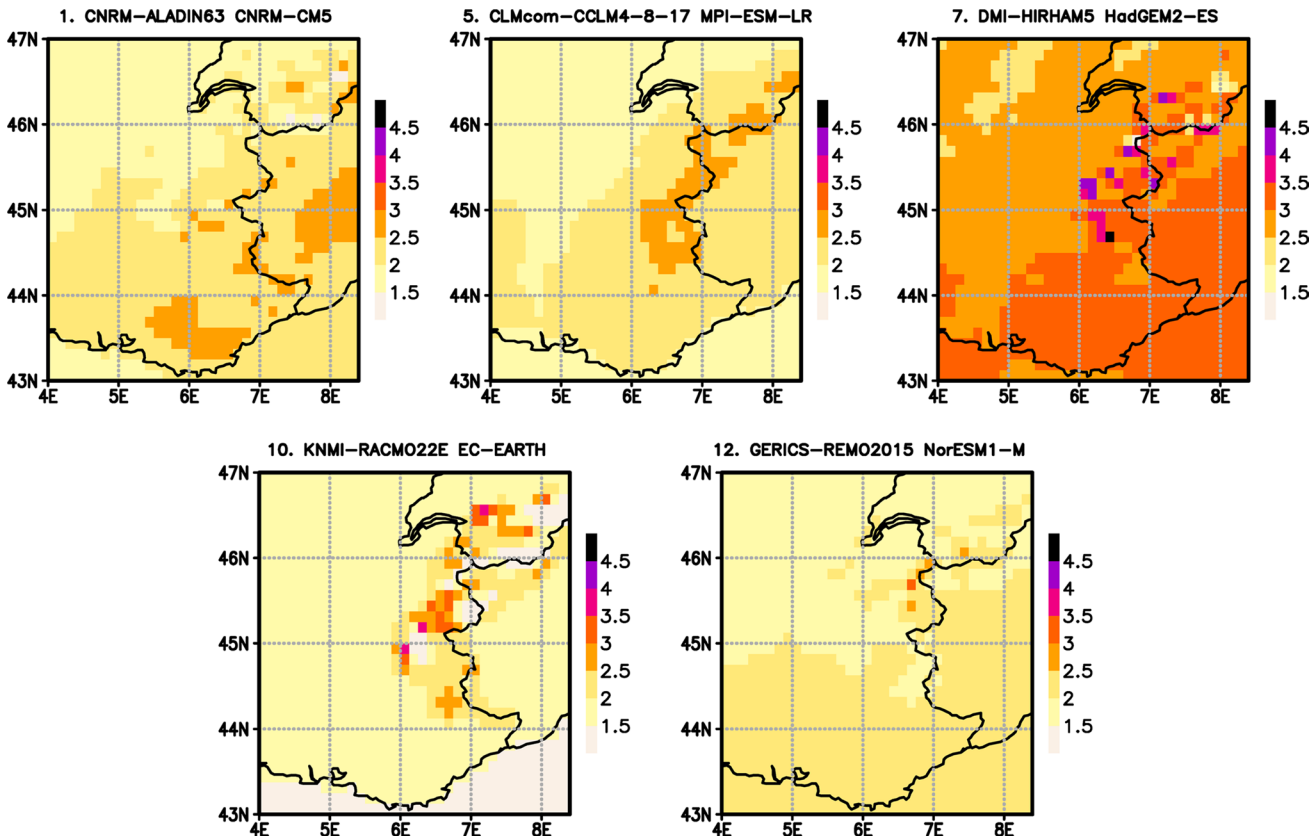

Fig. 12 Projected change in June-August mean surface air temperature (in °C) from 1981–2010 to 2070–2099 under RCP4.5 over the western Alps in the five EURO-CORDEX simulations identified in the figure headings. The ordinal numbers 1, 5, 7, 10 and 12 refer to Table 1. In contrast to the other temperature responses maps, in this figure the shading interval is 0.5°C

in Fig. 12 indicate that there is still room for investment in the development of RCMs.

Supplementary Information The online version contains supplementary material available at https://doi.org/10.1007/s00382-024-07258-3.

Acknowledgements Climate model output data have been downloaded from the Earth System Grid Federation web server: https://esgf-data.dkrz.de/search/esgf-dkrz/ (CORDEX runs) and https://esgf-data.dkrz.de/search/cmip6-dkrz/ (CMIP6 runs). Computing resources were provided by the Centre for Scientific Computing (CSC), Finland. Anonymous reviewer B is thanked for multiple interesting suggestions that have substantially widened the study.

Author Contributions The basic idea of the GCM-RCM hybrid method was suggested by JR and developed further by KR. KR performed the analyses and wrote the original draft of the manuscript. JR supported in editing the draft. Both authors have read and approved the final version.

Funding Open access funding provided by Finnish Meteorological Institute. The work was funded by the Tapsi project of the Lähi-Tapiola insurance company and by the Academy of Finland through the Finscapes project (decision no. 342561) and the Flagship funding (Grant no. 337549)

Availability of data and materials The model data are available in the Earth System Grid Federation (ESGF) data archive https://esgf-data.dkrz.de/search/cmip6-dkrz/ (CMIP6 GCMs) and https://esgf-data.dkrz.de/search/esgf-dkrz/ (CORDEX RCMs). Files generated during the work are available in the METIS repository (https://fmi.b2share.csc.fi/records/f8d862cc5a6d421dbf0ac4f55442b8b6).

Declarations

Conflict of interest The authors have no relevant financial or non-financial interests to disclose.

Ethics approval Not applicable.

References

Boé J, Somot S, Corre L et al (2020a) Large discrepancies in summer climate change over Europe as projected by global and regional climate models: causes and consequences. Clim Dyn 54:2981–3002. https://doi.org/10.1007/s00382-020-05153-1

Boé J, Terray L, Moine MP et al (2020b) Past long-term summer warming over western Europe in new generation climate models: role of large-scale atmospheric circulation. Environ Res Lett 15:084038. https://doi.org/10.1088/1748-9326/ab8a89

Boé J, Mass A, Deman J (2023) A simple hybrid statistical-dynamical downscaling method for emulating regional climate models over Western Europe. Evaluation, application, and role of added value? Clim Dyn 61:271–294. https://doi.org/10.1007/s00382-022-06552-2

Coppola E, Nogherotto R, Ciarlo JM et al (2021) Assessment of the European climate projections as simulated by the large EURO-CORDEX regional and global climate model ensemble. J Geophys Res Atmos 126:e2019JD032356. https://doi.org/10.1029/2019JD032356

Cui D, Liang S, Wang D (2021) Observed and projected changes in global climate zones based on Köppen climate classification. WIREs Clim Change 12:e701. https://doi.org/10.1002/wcc.701

Erlandsen HB, Parding KM, Benestad R et al (2020) A hybrid downscaling approach for future temperature and precipitation change. J Appl Meteorol Climatol 59:1793–1807. https://doi.org/10.1175/JAMC-D-20-0013.1

Giorgi F (2019) Thirty years of regional climate modeling: where are we and where are we going next? J Geophys Res Atmos 124:5696–5723. https://doi.org/10.1029/2018JD030094

Giorgi F, Torma C, Coppola E et al (2016) Enhanced summer convective rainfall at Alpine high elevations in response to climate warming. Nat Geosci 9:584–589. https://doi.org/10.1038/ngeo2761

IPCC (2021) Climate Change 2021: The Physical Science Basis. In: Masson-Delmotte V, Zhai P, Pirani A, Connors SL, Péan C, Berger S, Caud N, Chen Y, Goldfarb L, Gomis MI, Huang M, Leitzell K, Lonnoy E, Matthews JBR, Maycock TK, Waterfield T, Yelekci O, Yu R, Zhou B (eds) Contribution of working group I to the sixth assessment report of the intergovernmental panel on climate change. Cambridge University Press

Jacob D, Petersen J, Eggert B et al (2014) EURO-CORDEX: new high-resolution climate change projections for European impact research. Reg Environ Change 14:563–578. https://doi.org/10.1007/s10113-013-0499-2

Jacob D, Teichmann C, Sobolowski S et al (2020) Regional climate downscaling over Europe: perspectives from the EURO-CORDEX community. Reg Environ Change 20:51. https://doi.org/10.1007/s10113-020-01606-9

Klaver R, Haarsma R, Vidale PL et al (2020) Effective resolution in high resolution global atmospheric models for climate studies. Atmos Sci Lett 21:e952. https://doi.org/10.1002/asl.952

Lenderink G, van Ulden A, van den Hurk B et al (2007) A study on combining global and regional climate model results for generating climate scenarios of temperature and precipitation for the Netherlands. Clim Dyn 29:157–176. https://doi.org/10.1007/s00382-007-0227-z

Lenderink G, de Vries H, van Meijgaard E et al (2023) A perfect model study on the reliability of the added small-scale information in regional climate change projections. Clim Dyn 60:2563–2579. https://doi.org/10.1007/s00382-022-06451-6

Li G, Zhang X, Zwiers F et al (2012) Quantification of uncertainty in high-resolution temperature scenarios for North America. J Clim 25:3373–3389. https://doi.org/10.1175/JCLI-D-11-00217.1

Lind P, Belušić D, Médus E et al (2023) Climate change information over Fenno-Scandinavia produced with a convection-permitting climate model. Clim Dyn 61:519–541. https://doi.org/10.1007/s00382-022-06589-3

Liu P, Tsimpidi AP, Hu Y et al (2012) Differences between downscaling with spectral and grid nudging using WRF. Atmos Chem Phys 12:3601–3610. https://doi.org/10.5194/acp-12-3601-2012

Olesen M, Christensen JH, Kaas E et al (2018) Robustness of high-resolution regional climate projections for Greenland: a method

for uncertainty distillation. Clim Res 76:253–268. https://doi.org/10.3354/cr01536

O'Neill BC, Tebaldi C, van Vuuren DP et al (2016) The scenario model intercomparison project (ScenarioMIP) for CMIP6. Geosci Model Dev 9:3461–3482. https://doi.org/10.5194/gmd-9-3461-2016

Palmer TE, Booth BBB, McSweeney CF (2021) How does the CMIP6 ensemble change the picture for European climate projections? Environ Res Lett 16:094042. https://doi.org/10.1088/1748-9326/ac1ed9

Pietikäinen JP, Markkanen T, Sieck K et al (2018) The regional climate model REMO (v2015) coupled with the 1-D freshwater lake model FLake (v1): Fenno-Scandinavian climate and lakes. Geosci Model Dev 11:1321–1342. https://doi.org/10.5194/gmd-11-1321-2018

Räisänen J, Hansson U, Ullerstig A et al (2004) European climate in the late twenty-first century: regional simulations with two driving global models and two forcing scenarios. Clim Dyn 22:13–31. https://doi.org/10.1007/s00382-003-0365-x

Ruosteenoja K, Räisänen J, Pirinen P (2011) Projected changes in thermal seasons and the growing season in Finland. Int J Climatol 31:1473–1487. https://doi.org/10.1002/joc.2171

Stolpe MB, Cowtan K, Medhaug I et al (2021) Pacific variability reconciles observed and modelled global mean temperature increase since 1950. Clim Dyn 56:613–634. https://doi.org/10.1007/s00382-020-05493-y

Taranu IS, Somot S, Alias A et al (2023) Mechanisms behind large-scale inconsistencies between regional and global climate model-based projections over Europe. Clim Dyn 60:3813–3838. https://doi.org/10.1007/s00382-022-06540-6

Torma C, Giorgi F, Coppola E (2015) Added value of regional climate modeling over areas characterized by complex terrain—precipitation over the Alps. J Geophys Res Atmos 120:3957–3972. https://doi.org/10.1002/2014JD022781

von Storch H, Langenberg H, Feser F (2000) A spectral nudging technique for dynamical downscaling purposes. Mon Weather Rev 128:3664–3673. https://doi.org/10.1175/1520-0493(2000)128$<$3664:ASNTFD$>$2.0.CO;2